Synthesis and Characterization of δ-Atracotoxin-Ar1a, the Lethal Neurotoxin from Venom of the Sydney Funnel-Web Spider (*Atrax robustus*)†

Dianne Alewood,‡ Liesl C. Birinyi-Strachan,§ Paul K. Pallaghy,||,⊥ Raymond S. Norton,||,# Graham M. Nicholson,*,§ and Paul F. Alewood*,‡

Institute for Molecular Bioscience, University of Queensland, Queensland 4072 Australia, Department of Health Sciences, University of Technology Sydney, Broadway, New South Wales 2007, Australia, and Biomolecular Research Institute, Parkville, Victoria 3052, Australia

Received April 15, 2003; Revised Manuscript Received August 5, 2003

ABSTRACT: δ-Atracotoxin-Ar1a (δ-ACTX-Ar1a) is the major polypeptide neurotoxin isolated from the venom of the male Sydney funnel-web spider, *Atrax robustus*. This neurotoxin targets both insect and mammalian voltage-gated sodium channels, where it competes with scorpion α-toxins for neurotoxin receptor site-3 to slow sodium-channel inactivation. Progress in characterizing the structure and mechanism of action of this toxin has been hampered by the limited supply of pure toxin from natural sources. In this paper, we describe the first successful chemical synthesis and oxidative refolding of the four-disulfide bond containing δ-ACTX-Ar1a. This synthesis involved solid-phase Boc chemistry using double coupling, followed by oxidative folding of purified peptide using a buffer of 2 M GdnHCl and glutathione/glutathiol in a 1:1 mixture of 2-propanol (pH 8.5). Successful oxidation and refolding was confirmed using both chemical and pharmacological characterization. Ion spray mass spectrometry was employed to confirm the molecular weight. ^{1}H NMR analysis showed identical chemical shifts for native and synthetic toxins, indicating that the synthetic toxin adopts the native fold. Pharmacological studies employing whole-cell patch clamp recordings from rat dorsal root ganglion neurons confirmed that synthetic δ-ACTX-Ar1a produced a slowing of the sodium current inactivation and hyperpolarizing shifts in the voltage-dependence of activation and inactivation similar to native toxin. Under current clamp conditions, we show for the first time that δ-ACTX-Ar1a produces spontaneous repetitive plateau potentials underlying the clinical symptoms seen during envenomation. This successful oxidative refolding of synthetic δ-ACTX-Ar1a paves the way for future structure−activity studies to determine the toxin pharmacophore.

The venom of the male Sydney funnel-web spider, *Atrax robustus* (*Mygalomorphae*:*Hexathelidae*:*Atracinae*) contains a potent neurotoxin δ-ACTX-Ar1a[1] (formerly robustoxin; Figure 1A,B) that has been responsible for a number of human fatalities (*1*, *2*). Previous studies have shown that this toxin slows sodium-channel inactivation (*3*) by binding to receptor site-3 on the sodium channel (*4*), although the precise effects on neuronal excitability have not been determined. An antivenom (*5*) has been used successfully since 1980 in severe cases of envenomation by *A. robustus* and other Australian funnel-web species to reverse life-threatening cardiorespiratory collapse (*6*). The antivenom is raised against total milked male venom rather than the isolated toxin. Unfortunately, venom collection is a laborious, costly, and dangerous process, not to mention that there is limited availability and poor survival of male spiders in long-term captivity. Supplies of pure toxin would therefore be of great benefit for further studies of the structure and mechanism of action of this potent toxin.

Early attempts at the isolation of δ-ACTX-Ar1a and subsequent sequence determination gave conflicting and incorrect results (*7*, *8*). The advent of more reliable analysis methods resulted in a proposed amino acid sequence of 42

† This work was supported in part by the Australian Research Council.

* To whom correspondence should be addressed. (P.F.A.) Fax: +617 3346-2101. Phone: +617 3346-2982. E-mail: P.Alewood@imb.uq.edu.au. (G.M.N.) Fax: +612 9514-2230. Phone: +612 9514-2228. E-mail: Graham.Nicholson@uts.edu.au.

‡ University of Queensland.

§ University of Technology Sydney.

|| Biomolecular Research Institute.

⊥ Present address: Department of Biochemistry and Molecular Biology, The University of Melbourne, Victoria 3010, Australia.

Present address: Walter and Eliza Hall Institute of Medical Research, Parkville, Victoria 3052, Australia.

[1] Abbreviations: Aah II, α-toxin II from the venom of the scorpion *Androctonus australis hector*; Aah IT, insect-selective neurotoxin from the venom of the scorpion *Androctonus australis hector*; δ-ACTX-Ar1a, δ-atracotoxin-Ar1a from the venom of the Sydney funnel-web spider *Atrax robustus*; δ-ACTX-Hv1a, δ-atracotoxin-Hv1a from the venom of the Blue Mountains funnel-web spider *Hadronyche versuta*; Boc, *tert*-butyloxycarbonyl; BrZ, bromobenzyloxycarbonyl; Bzl, benzyl; CHO, formyl; ClZ, chlorobenzyloxycarbonyl; CnERG1, HERG K^+ channel blocker from the venom of the scorpion *Centruroides noxius*; DCM, dichloromethane; DMF, dimethylformamide; DRG, dorsal root ganglia; 4-MeBzl, 4-methylbenzyl; GdnHCl, guanidinium hydrochloride; ICK, inhibitory cystine knot; IS-MS, ionspray mass spectrometry; NMR, nuclear magnetic resonance; OcHex, *O*-cyclohexyl; Pam, phenylacetamidomethyl; PLTX II, insect-selective neurotoxin from the venom of the spider *Plectreurys tristis*; RP-HPLC, reversed-phase high-performance liquid chromatography; SPPS, solid-phase peptide synthesis; TCEP, triscarboxyethylphosphine; TEA, tetraethylammonium; TFA, trifluoroacetic acid; TFE, trifluoroethanol; TOCSY, total correlation spectroscopy; Tos, tosyl; TTX, tetrodotoxin.

10.1021/bi030091n CCC: $25.00
Published on Web 10/16/2003

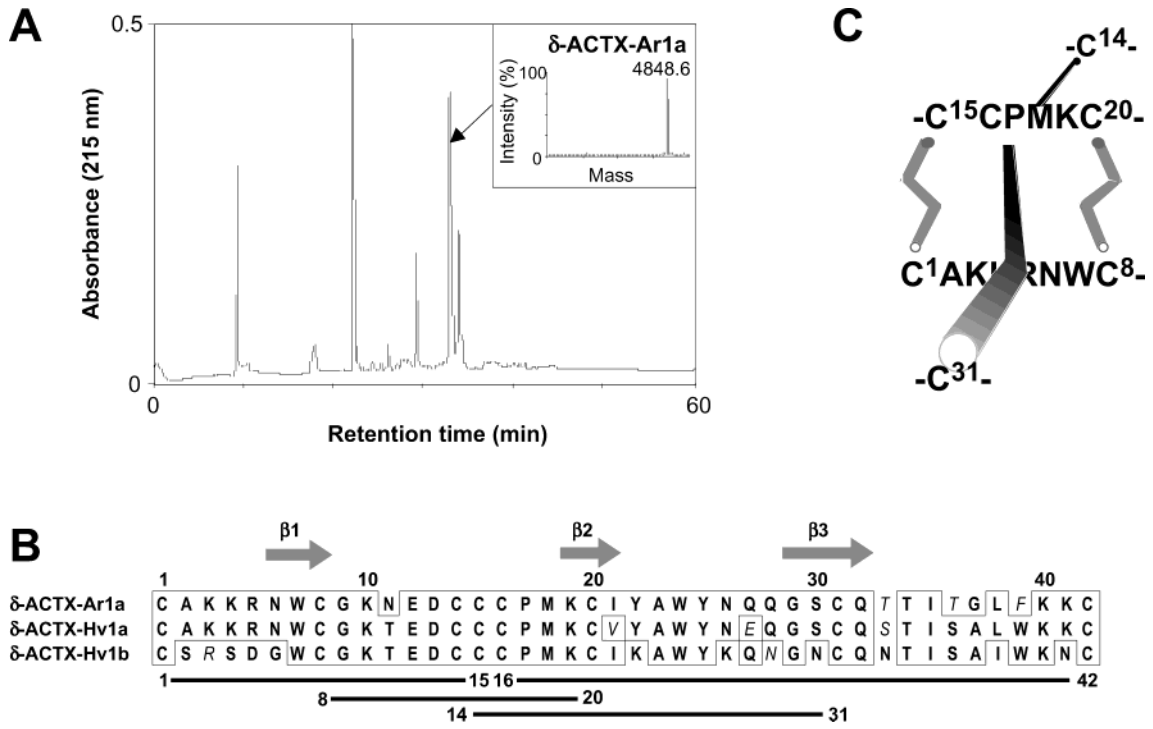

FIGURE 1: (A) LCMS trace of whole milked male Sydney funnel-web (*A. robustus*) venom with the location of δ-ACTX-Ar1a shown. The reconstructed IS-MS data for the δ-ACTX-Ar1a C_{18} RP-HPLC peak are shown in the inset. (B) Sequence comparison of δ-atracotoxins (δ-ACTX). Identical residues are boxed, and conservative substitutions are shown in italics. The disulfide bonding pattern is indicated below the sequence. Secondary structure for δ-ACTX-Ar1a is shown at the top of the figure where arrows represent β-strands. (C) The cystine knot of δ-ACTX-Ar1a in which the embedded ring formed by the two disulfide bonds Cys^1-Cys^{15} and Cys^8-Cys^{20} is penetrated by a third disulfide bond $Cys^{14}-Cys^{31}$.

residues containing eight cysteines (*9*). The cysteine framework proposed by Fletcher et al. (*10*) (Figure 1B) is unique in bioactive peptides due to the occurrence of three contiguous cysteines ($Cys^{14,15,16}$) and cysteines at both the N- and the C-termini. Similar peptides have subsequently been found in the venom of other Australian funnel-web spiders (e.g., δ-ACTX-Hv1a (formerly versutoxin) and δ-ACTX-Hv1b from *Hadronyche versuta* (*11*, *12*) (Figure 1B)). The disulfide connectivity of δ-ACTX-Ar1a corresponds to a 1−4, 2−6, 3−7, 5−8 motif that has also been observed in the venom of snakes (echistatin) (*13*) and scorpions (Aah IT, chlorotoxin) (*14*), but none of these other toxins has the same cysteine spacings as δ-ACTX-Ar1a. δ-ACTX-Ar1a has sequence and structural similarities with a number of other spider and marine snail toxins (ω-ACTX-Hv1, ω-agatoxin IVB, ω-agatoxin I, ω-conotoxin GVIA, huwentoxin) (*15*) and a plant polypeptide (gurmarin) (*16*), all of which have six conserved cysteine residues. This group of toxins conform to a common structural motif, referred to as the inhibitory cystine knot (ICK) motif (*17*). The activities of this group of compounds are quite diverse with activity at the voltage-gated sodium channel, voltage-gated calcium channel, the nicotinic acetylcholine receptor, and the signal transduction pathway for the sweet-taste receptor.

The synthesis of polypeptides around 20−30 residues in length and with three disulfide bonds is now carried out routinely by a number of groups with good results. Even some peptides with four disulfides such as the structurally related J-ACTX-Hv1c (36 residues) can be folded with high efficiency whether the toxin is produced recombinantly in *Escherichia coli* (*18*) or via SPPS techniques (King, G. F., personal communication). However, the synthesis of longer polypeptide toxins with four or more disulfide bonds is generally more demanding. The spider toxins, ω-agatoxin IVA (48 residues, 4 disulfides) (*19*) and PLTX II (44 residues, 5 disulfides) (*20*), and the snake toxin calciseptine (60 residues, 4 disulfides) (*21*) have been assembled using segment condensation methods, while the scorpion toxin, maurotoxin (34 residues, 4 disulfides) (*22*), was assembled using SPPS techniques. The oxidation conditions required to obtain each of these toxins were very different. While crude, reduced maurotoxin was easily oxidized under basic conditions in air at room temperature in 48 h, the oxidation of pure, reduced ω-agatoxin IVA could only be achieved at a low temperature after the addition of 20% glycerol and a redox shuffling system. The oxidation of pure, reduced PLTX II was finally achieved in 50% 2-propanol buffer, pH 8.5, in a redox shuffling system at 30 °C after exhaustive oxidation trials. Studies on the reoxidation of pure, reduced Aah II (64 residues, 4 disulfides) (*23*) from scorpion toxin also demonstrated that very specific oxidation conditions are often required to obtain a good yield of the desired product.

We have shown previously that it is possible to synthesize polypeptides in good yields using SPPS, Boc/TFA chemistry protocols (e.g., HIV-1 protease (99-residue enzyme of HIV-1) (*24*), CnERG1 (HERG K^+ channel blocker from scorpion venom) (*25*) and EETI-II (*Ecballium elaterium*-II, multiply disulfide bonded trypsin inhibitor) (*26*)) and have used similar methods to synthesize δ-ACTX-Ar1a. Using ^1H NMR and whole-cell patch clamp experiments, we confirmed that synthetic δ-ACTX-Ar1a has a native sequence, disulfide pairings, and fold (*27*) and modulates voltage-gated sodium-channel function in a manner similar to the native toxin (*3*). The availability of synthetic toxin has allowed us to further

explore the biological activity of the toxin, resulting in the observation that δ-ACTX-Ar1a causes repetitive firing and prolongation of the action potential. These actions underlie the clinical symptoms seen during envenomation and further contribute to our understanding of the molecular basis for activity of this potent neurotoxin on voltage-gated sodium channels.

MATERIALS AND METHODS

Materials. Protected Boc-amino acid derivatives were from Peptide Institute (Osaka, Japan) or Applied Biosystems (ABI, Melbourne, Australia). The following side-chain protected amino acids were used: Arg(Tos), Asp(OcHex), Cys(4-MeBzl), Glu(OcHex), Trp(CHO), Lys(ClZ), Ser(Bzl), Thr-(Bzl), and Tyr(BrZ). All other Boc-amino acids were unprotected. Dimethylformamide (DMF), dichloromethane (DCM), diisopropylethylamine (DIEA), trifluoroacetic acid (TFA), dicyclohexylcarbodiimide (DCC), and hydroxybenzotriazole (HOBT), all peptide synthesis grade, were supplied by Auspep Pty. Ltd. (Melbourne, Australia). HPLC-grade acetonitrile and methanol were supplied by Millipore Waters. Boc-Cys(4MeBzl)-OCH_2-Pam resin (0.66 mmol/g) was supplied by Applied Biosystems. *p*-Cresol and *p*-thiocresol were of the highest grade available from Fluka (Germany). Tetrodotoxin (TTX) was obtained from Calbiochem.

Peptide Synthesis. The chain assembly of the peptide was performed on a modified ABI 430A peptide synthesizer using symmetric anhydride and active ester chemistry to couple the Boc-protected amino acid to the deprotected resin. The Boc protecting group was removed using 100% TFA, and DMF was used as both the coupling solvent and for flow washes throughout the cycle (*28*). Each residue was routinely doubly coupled. The progress of the assembly was monitored by quantitative ninhydrin monitoring (*29*).

Prior to HF cleavage, the N_α-Boc group was removed using TFA to prevent side reactions in subsequent steps, and then the formyl side-chain protecting group on Trp was removed using a solution of ethanolamine (1.5 g) in 5% water/DMF (25 mL). Finally, the peptide resin was washed with DMF and DCM and dried under nitrogen. Cleavage from the resin and the simultaneous deprotection of the remaining side-chain protecting groups was carried out in an HF cleavage apparatus supplied by the Peptide Institute, using a ratio of 9:1 HF to scavengers (1:1 *p*-cresol/*p*-thiocresol) for 1.5 h at −7 to −2 °C. After the removal of HF, the peptide was precipitated with cold ether, filtered, washed with more ether, and then dissolved with TFA. The solution was then diluted to 1−2% TFA with water and lyophilized.

Mass Spectrometry. Mass analyses were performed on a PE-Sciex API III ion spray mass spectrometer (IS-MS) over 300−2000 amu at a mass accuracy of ±0.2 amu and an orifice potential of 90 V. The peptide (1 mg/mL) was dissolved in 45% acetonitrile in water containing 0.1% TFA and then introduced to the spectrometer via a glass capillary using either an infusion of the peptide solution at a flow rate of 5 μL/min or by injection of a 5-μL sample via an injection loop into a flow of 50% acetonitrile in water plus 0.01% formic acid delivered to the spectrometer at 30−50 μL/min.

Chromatographic Purification, Folding, and Oxidation. The crude, reduced peptide was examined by RP-HPLC, and the correct molecular weight was confirmed by IS-MS. An Ellman's test (*30*) was carried out to confirm the presence of free sulfhydryl groups.

Purification of the crude reduced peptide was carried out by dissolving the peptide in unbuffered 6 M GdnHCl (5 mL) and then loading it onto a Vydac C_4 preparative column. Following washing to remove the GdnHCl, the column was eluted with a gradient from 0 to 80% buffer B (0.1%TFA/acetonitrile) over 80 min with a linear gradient. Fractions were examined by IS-MS for correct mass and HPLC for purity and coelution and combined where appropriate prior to lyophilization.

Prior to oxidation, the pure reduced peptide (2.3 μmol) was dissolved in 500 μL of unbuffered 6 M GdnHCl and then immediately diluted to 5 μM in 50% 2-propanol/0.66 M ammonium acetate buffer, pH 8.0, containing 2 M GdnHCl and glutathione/glutathiol (1:10). This mixture was then stirred at 4 °C for 7 days in silanized glassware. Completion of the oxidation was confirmed by mass analysis of a peak that coeluted with native δ-ACTX-Ar1a using an analytical Vydac C_4 300-Å column (4.6 × 250 mm) with a gradient from 0 to 67% buffer B (0.1%TFA/acetonitrile) at 1 mL/min over 60 min. UV detection was at 215 nm.

After acidification and dilution to <5% 2-propanol, the oxidation mixture was loaded directly onto a Vydac C_4 preparative chromatography column. The column was eluted with buffer A (0.1%TFA/water) until complete elution of the buffer/guanidine solution and then eluted using a linear gradient of 0−80% buffer B (0.1%TFA/acetonitrile) over 80 min at a flow rate of 8 mL/min. Fractions containing the pure product were identified using analytical RP-HPLC and IS-MS and then combined and lyophilized.

NMR Spectroscopy. ^{1}H NMR spectra were recorded on δ-ACTX-Ar1a prepared from *A. robustus* venom, as described previously (*15*), and the chemically synthesized form described in this paper. A 0.5-mg sample of synthetic δ-ACTX-Ar1a was dissolved in 300 μL of 90% H_2O/10% ^2H_2O, pH 5.0, and placed in a susceptibility-matched 5-mm NMR tube designed for low sample volumes (Shigemi, Tokyo). One-dimensional ^{1}H NMR spectra and 2-D TOCSY spectra were acquired on synthetic δ-ACTX-Ar1a at 3 °C using the WATERGATE scheme and a 3−9−19 selective pulse for water suppression (*31*) on Bruker AMX-500 and DRX-600 spectrometers, respectively, and were processed and analyzed using protocols described previously (*15*). The spin lock time for the TOCSY was 70 ms.

Electrophysiological Studies. Acutely dissociated dorsal root ganglion (DRG) neurons were prepared from 4 to 12 day-old Wistar rats and maintained in a short-term primary culture as previously described (*32*). Current- and voltage-clamp recordings were made using an Axopatch 200A patch-clamp amplifier (Axon Instruments, Foster City, CA) and whole-cell patch-clamp techniques (*33*). Micropipets were pulled from borosilicate glass capillary tubing (Corning 7052 Glass, Warner Instruments) and had dc resistances of 0.8−2.0 MΩ.

To record sodium currents, pipets were filled with a solution of the following composition (in mM): CsF 135; NaCl 10; and *N*-2-hydroxyethylpiperazine-*N*-2-ethanesulfonic acid (HEPES) 5, with the pH adjusted to 7.0 with 1 M CsOH. The external solution contained (in mM): NaCl 30; $MgCl_2$ 1; $CaCl_2$ 1.8; CsCl 5; KCl 5; D-glucose 25; HEPES

5; tetraethylammonium (TEA) chloride 20; and tetramethylammonium chloride 70, with the pH adjusted to 7.4 with 1 M TEA hydroxide.

To record resting and action potentials, pipets were filled with a solution of the following composition (in mM): KCl 135; NaCl 10; and HEPES 5, with the pH adjusted to 7.0 with 1 M KOH. The external solution contained (in mM): NaCl 100; $MgCl_2$ 1; $CaCl_2$ 1.8; KCl 5; D-glucose 25; and HEPES 5, with the pH adjusted to 7.4 with 1 M NaOH. Action potentials were elicited by 1−2 ms supramaximal currents delivered at 0.1 Hz. Cells were rejected if the resting membrane potentials were less than −50 mV.

In voltage-clamp experiments, the holding potential was −80 mV, and the sodium concentration in the external solution was reduced to 30 mM to improve series resistance compensation and to avoid saturation in the recording system (*34*). The liquid junction potential between internal and external solutions was approximately −6 mV, and all data were compensated for this value.

Large round light DRG cells with diameters of 20−40 μm were selected for experiments. Larger cells from older animals tended to express fast tetrodotoxin (TTX)-sensitive sodium currents, while smaller cells tended to express predominantly slow TTX-resistant sodium currents (*35*). In experiments that assessed the actions of δ-ACTX-Ar1a on TTX-resistant currents, 200 nM TTX was applied in the external solution to eliminate any residual TTX-sensitive sodium currents. The experiments used in this study were rejected if there were large leak currents or if currents showed signs of poor space clamping such as an abrupt activation of currents upon relatively small depolarizing pulses. Data were filtered at 5 kHz (four-pole low-pass Bessel filter), and digital sampling rates were between 15 and 25 kHz depending on the voltage protocol length. Leakage and capacitive currents were digitally subtracted with $P-P/4$ procedures (*36*), and the series resistance compensation was >80% for all cells.

The curve fits for the I/V data were obtained using the following equation:

$$I_{Na} = g_{max}\left(1 - \frac{1}{1 + \exp((V - V_{1/2})/s)}\right)(V - V_{rev}) \quad (1)$$

where I_{Na} is the amplitude of the peak sodium current at a given test potential, V; g_{max} is the maximal sodium conductance; V_{rev} is the reversal potential; $V_{1/2}$ is the voltage at half-maximal activation; and s is the slope factor.

The fitted curves for steady-state sodium current inactivation (h_∞) were obtained using the following form of the Boltzmann equation:

$$h_\infty = \frac{1 - C}{1 + \exp[(V - V_{1/2})/k]} + C \quad (2)$$

where $V_{1/2}$ is the voltage at half-maximal inactivation; k is the slope factor; V is the test potential; and C is a constant or noninactivating fraction (usually zero in controls).

Comparisons of two sample means were made using the Student's t-test. A test was considered to be significant when $P < 0.05$. All data are presented as mean ± standard error of the mean (SEM).

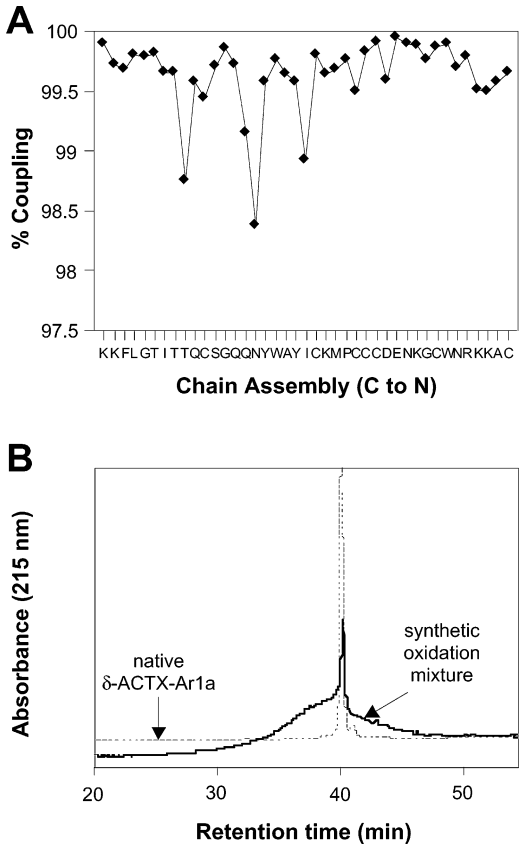

FIGURE 2: (A) Percent coupling yields for the chain assembly of δ-ACTX-Ar1a after a single coupling. (B) Coelution of native δ-ACTX-Ar1a and the major product from oxidation of reduced δ-ACTX-Ar1a on C_{18} RP-HPLC.

RESULTS

Synthesis. The chain assembly of the peptide proceeded without major difficulty, although several residues were only 98.5% incorporated after the first coupling (Figure 2A). Each of these couplings increased to 99.5% after the second coupling with an average coupling yield of 99.79% for the total synthesis. The overall assembly yield was 92% desired peptide. Purification of the crude peptide resulted in 90% pure peptide (plus minor deletion products that could not be removed without major product loss) that was used for the oxidation studies and the final large-scale oxidation. The recovery from the large-scale oxidation (10−15%) was poor due to the strong tendency of this toxin to adhere to glass and plastic surfaces and to the reversed-phase column.

The synthetic toxin coeluted with native toxin on a C_4 RP-HPLC column using a 0−67% acetonitrile linear gradient at 1 mL/min over 60 min (Figure 2B). The synthetic toxin had an identical mass with the native toxin (M_r native toxin = 4848.7 Da; M_r synthetic toxin = 4848.8 ± 0.6 Da) (Figure 3).

NMR Spectroscopy. The amide and aromatic regions of the 1-D ^{1}H NMR spectra of native and synthetic δ-ACTX-Ar1a are shown in Figure 4A. The spectra are identical, including the chemical shifts of the broad tyrosine hydroxyl protons at 9.04 and 9.86 ppm (*27*). There is a sharp peak at 8.42 ppm in synthetic δ-ACTX-Ar1a that is absent in native δ-ACTX-Ar1a and sharp peaks at 7.08 and 7.17 ppm for native δ-ACTX-Ar1a that are reduced in intensity for synthetic δ-ACTX-Ar1a. As there are no corresponding

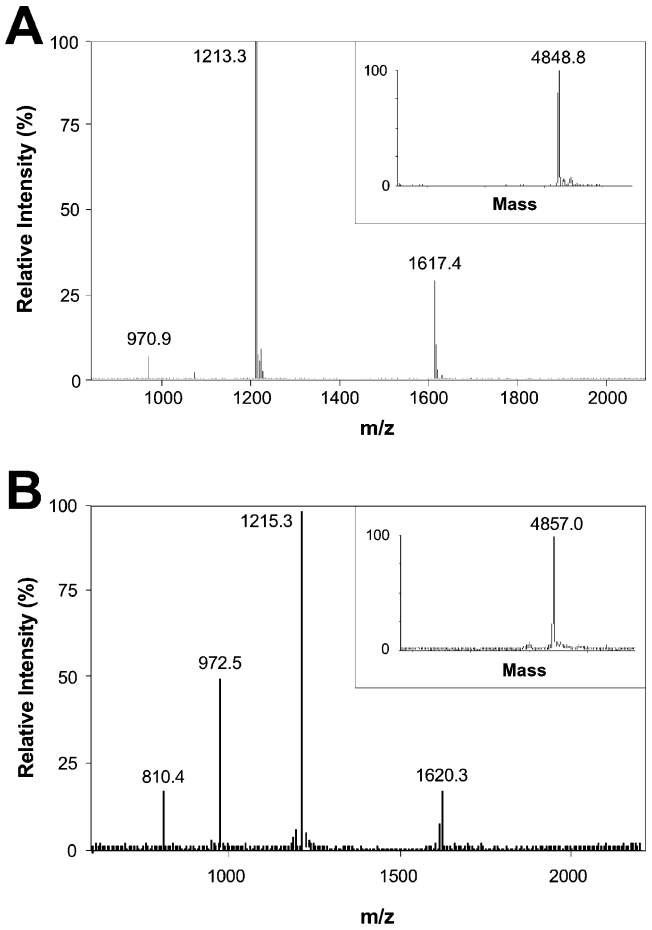

FIGURE 3: IS-MS for reduced (A) and oxidized (B) δ-ACTX-Ar1a. Insets show the reconstructed masses.

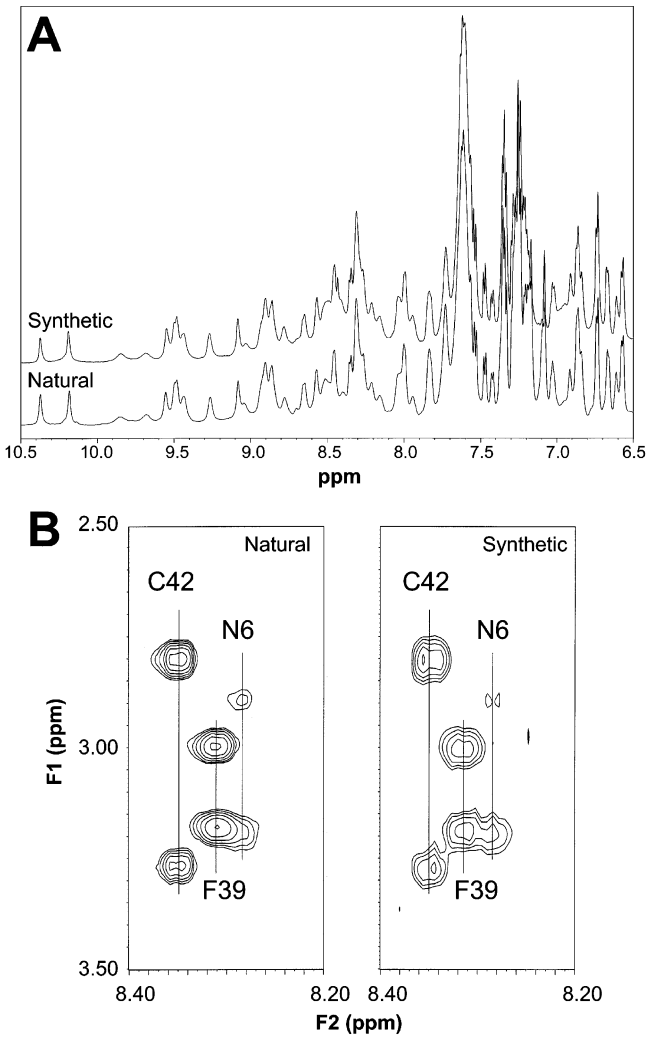

FIGURE 4: Comparison of synthetic and native δ-ACTX-Ar1a by NMR. (A) One-dimensional ^{1}H NMR spectra (500 MHz) of native and synthetic δ-ACTX-Ar1a showing amide/aromatic regions. (B) Sections of the 2-D TOCSY spectra (600 MHz) of native and synthetic δ-ACTX-Ar1a showing connectivities between the backbone amide and C$^\beta$H resonances.

cross-peaks for these resonances in the respective TOCSY spectra, we believe that they originate from low molecular weight impurities. Sections of the TOCSY spectra of native and synthetic δ-ACTX-Ar1a are shown in Figure 4B, which indicate that the chemical shifts for the C-terminal Cys[42] residue are essentially identical in the two samples.

Effects of Synthetic δ-ACTX-Ar1a on TTX-Sensitive and TTX-Resistant Sodium Currents in Rat DRG Neurons. Under voltage-clamp conditions, native δ-ACTX-Ar1a exerts a concentration-dependent reduction in the peak TTX-sensitive sodium current amplitude and slows the rate of sodium current inactivation (*3*). Figure 5A shows the effect of 30 nM synthetic δ-ACTX-Ar1a on TTX-sensitive sodium currents. Similarly to native toxin, synthetic δ-ACTX-Ar1a reduced the peak TTX-sensitive sodium current amplitude, although the extent of block with the synthetic toxin was typically slightly smaller. In addition, synthetic δ-ACTX-Ar1a, like native toxin, slowed the rate of the TTX-sensitive sodium current inactivation to a similar extent, as evidenced by a sustained current during depolarizing test potentials. At the end of the 50 ms depolarizing test pulse, this was 35.9 ± 4.6% of the control peak sodium current amplitude. The reduction in the sodium current amplitude and slowing of the current inactivation produced by both toxins was not reversible, even after prolonged washing with toxin-free solution. In marked contrast to its action on TTX-sensitive sodium channels, synthetic δ-ACTX-Ar1a (300 nM), like native toxin, failed to significantly alter either the amplitude or the timecourse of TTX-resistant sodium currents (data not shown).

Effects of Synthetic δ-ACTX-Ar1a on the Voltage Dependence of g_{Na} in Rat DRG Neurons. Previous studies have shown that native δ-ACTX-Ar1a shifts the threshold of activation of TTX-sensitive sodium currents in the hyperpolarizing direction (*3*). Comparison of the effects of synthetic δ-ACTX-Ar1a (Figure 5C) revealed similar hyperpolarizing shifts in the voltage dependence of activation (approximately 10 mV). Figure 5C also shows that these changes occurred in the absence of significant changes in reversal potential, which was decreased only slightly by 1 ± 1 mV for synthetic toxin ($n = 3$) as compared to 2 ± 1 mV for the native toxin (*3*, *4*, *39*).

The hyperpolarizing shift in the activation voltage suggested that, like native toxin, synthetic δ-ACTX-Ar1a affects the voltage dependence of activation; therefore, the effects of synthetic toxin on the voltage dependence of g_{Na} were examined. Fitting of the *I*/*V* data with a Boltzmann function revealed that 30 nM synthetic δ-ACTX-Ar1a caused a −7 mV shift in the voltage midpoint ($V_{1/2}$) from −36 ± 3 to

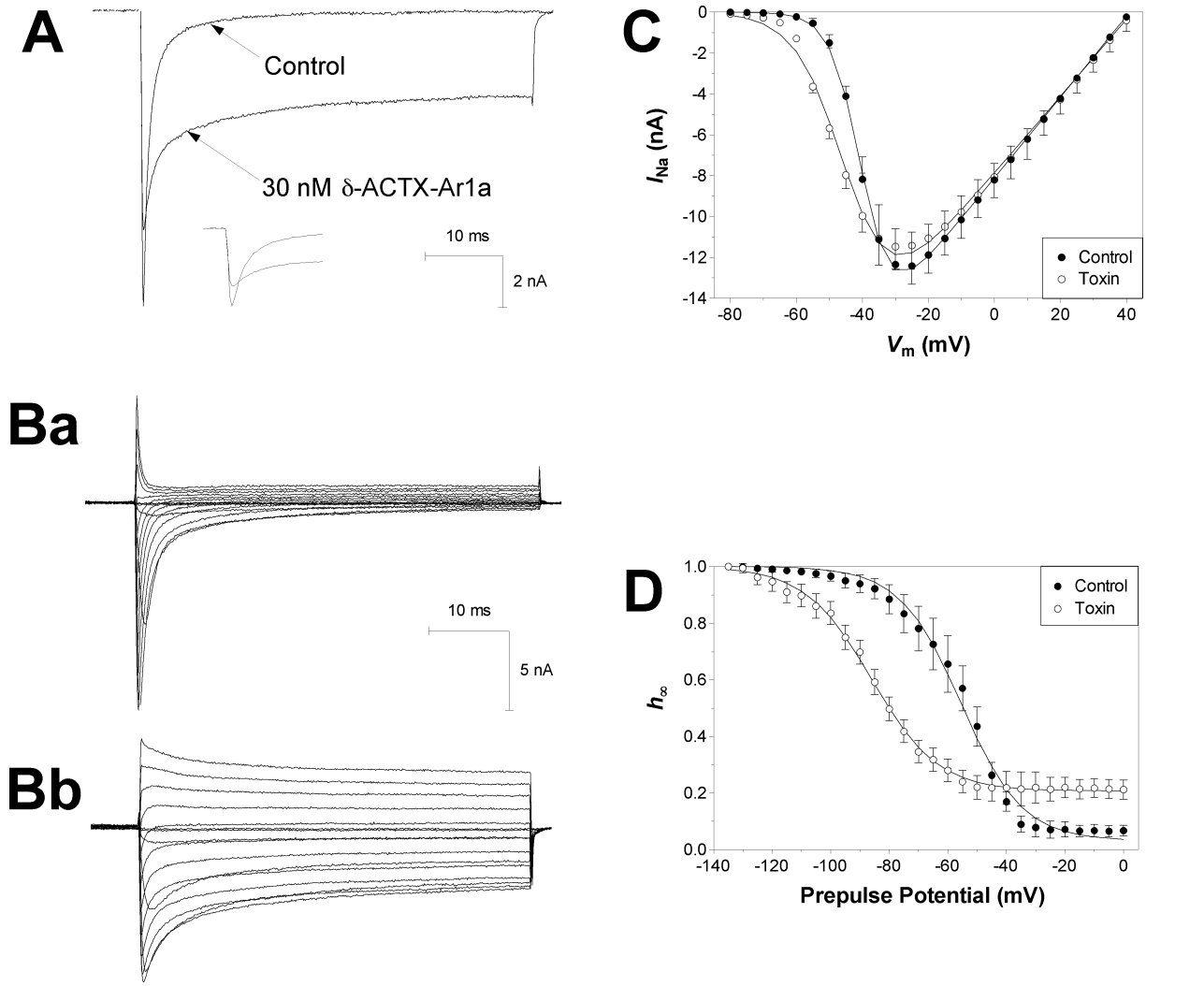

FIGURE 5: Typical effects of synthetic δ-ACTX-Ar1a on the gating and kinetics of TTX-sensitive sodium currents in rat DRG neurons. (A) Typical effects of synthetic δ-ACTX-Ar1a on the time course and amplitude of TTX-sensitive sodium currents. Sodium currents were evoked by a 50-ms depolarization to −10 mV applied every 10 s from a holding potential of −80 mV before, and 10 min after, the addition synthetic toxin. The inset shows the magnified peak TTX-sensitive sodium currents. (B) Typical effects of synthetic δ-ACTX-Ar1a on the voltage dependence of activation of TTX-sensitive sodium currents. Current responses before (Ba) and 10 min after (Bb) addition of 30 nM δ-ACTX-Ar1a were evoked by a series of 50-ms depolarizations from a holding potential of −80 mV. Test voltages ranged from −80 to +70 mV in 5-mV steps and were delivered every 10 s. For clarity, only data in 10 mV increments are shown. (C) Peak current/voltage relationships, determined from the data in panels Ba and Bb, are graphed in the absence (closed symbols) and presence (open symbols) of 30 nM synthetic δ-ACTX-Ar1a ($n = 3$). Data were then fitted with eq 1 as described in the Materials and Methods. (D) Typical effects of synthetic δ-ACTX-Ar1a on steady-state TTX-sensitive sodium current inactivation (h_∞). Steady-state inactivation was determined using a standard two-pulse protocol. Conditioning prepulse voltages of a 1-s duration ranging from −135 to 0 mV in 5-mV steps were followed by a 50-ms depolarizing test pulse to −10 mV delivered every 10 s. Peak TTX-sensitive sodium currents recorded during the test pulse are plotted against the prepulse potential, and the amount of sodium current that is available for activation during the test pulse under control conditions (closed symbols) and during toxin perfusion (open symbols) is shown ($n = 5$). Currents were normalized to the maximum control current and fitted according to eq 2 as described in the Materials and Methods.

−43 ± 4 mV ($P < 0.05$, $n = 3$), with no significant change in the slope factor. These shifts in $V_{1/2}$ were not statistically different from the −11 mV shift obtained with native δ-ACTX-Ar1a (*3*).

Effects of Synthetic δ-ACTX-Ar1a on the Voltage Dependence of Steady-State Sodium-Channel Inactivation (h_∞) in Rat DRG Neurons. Native δ-ACTX-Ar1a shifts the steady-state sodium-channel inactivation curve (h_∞/V) in the hyperpolarizing direction by 7 mV and produces a noninactivating component at depolarized prepulse test potentials (*3*). To quantify any such changes in the voltage dependence of steady-state sodium-channel inactivation produced by synthetic δ-ACTX-Ar1a, measurements were made with a standard two-pulse protocol, as detailed in Figure 5D. Peak sodium currents recorded during the test pulse were normalized to the maximum value and plotted against the conditioning prepulse potential. Curves were then fitted using eq 2 in the Materials and Methods. Similarly to native toxin, synthetic δ-ACTX-Ar1a caused a significant 22 mV ($n = 5$; $P < 0.02$) hyperpolarizing shift in the voltage at which half the sodium channels were inactivated ($V_{1/2}$), from −58 ± 3 to −80 ± 5 mV ($n = 3$) but with no change in the slope factor. In addition, 30 nM synthetic δ-ACTX-Ar1a exhibited a classical noninactivating component (21.5 ± 2.9% of the maximal sodium current, determined from *C* in eq 2 in the Materials and Methods) at prepulse test potentials more depolarized than −40 mV (see Figure 5D). This noninactivating component has been noted with other toxins

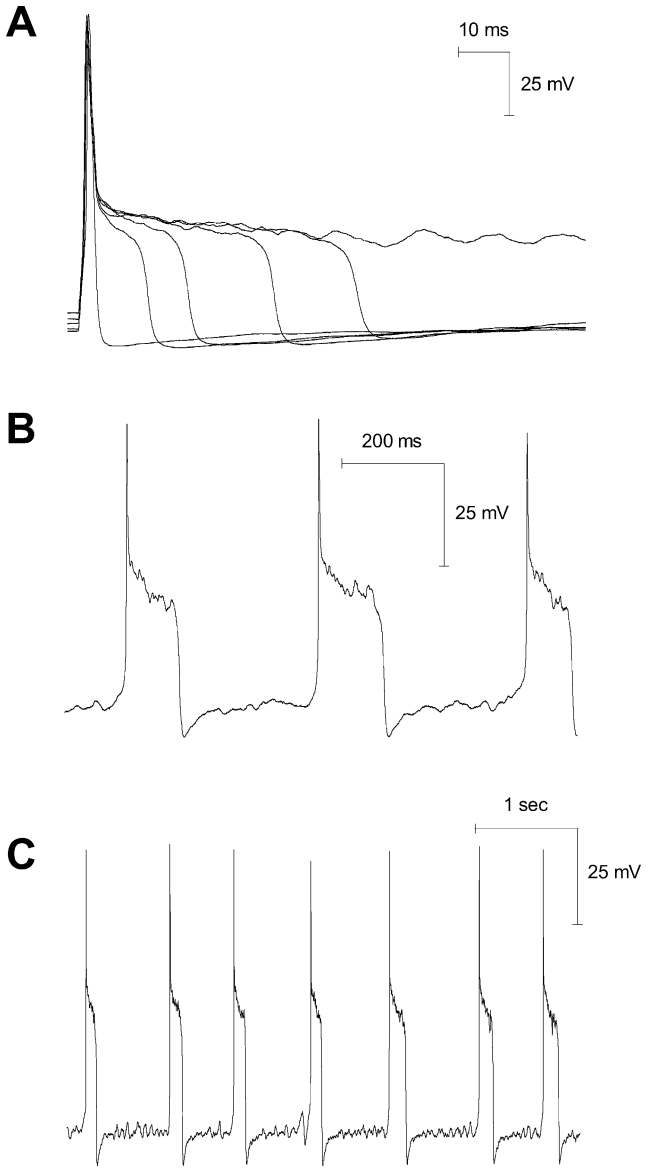

FIGURE 6: Typical effects of native and synthetic δ-ACTX-Ar1a on resting and action potentials from DRG neurons expressing TTX-S sodium currents. (A) Typical effects of synthetic δ-ACTX-Ar1a to increase the action potential duration. Action potentials were elicited by supramaximal current pulses of a 1-ms duration delivered every 10 s. Synthetic δ-ACTX-Ar1a markedly prolonged the repolarization phase of the action potential eventually leading to a plateau potential after at least 10 min. (B and C) Typical effects of synthetic δ-ACTX-Ar1a to induce spontaneous repetitive action potentials. Action potentials in these panels are not stimulus locked. Data are representative of $n = 5$ experiments.

interacting with neurotoxin receptor site-3 on the sodium channel (*32*, *37*, *38*).

Effects of Synthetic δ-ACTX-Ar1a on Resting and Action Potentials in Rat DRG Neurons. Limited supplies of δ-ACTX-Ar1a have previously prevented full characterization of the toxin on neuronal excitability. Using synthetic toxin under current-clamp conditions, δ-ACTX-Ar1a (30 nM) produced a prolongation of the repolarization phase of the action potential. Within 5−10 min, this resulted in the appearance of a plateau potential that lasted often up to 100 ms (Figure 6A−C). The plateau action potential progressively developed from a shoulder arising in the last half of the repolarizing phase. Perfusion of 30 nM synthetic δ-ACTX-Ar1a significantly increased the action potential duration (measured at 20% action potential height), almost 13-fold, after 5−10 min when compared to the control duration ($n = 7$; $P = 0.004$). The resting membrane potential (E_m), however, was not significantly altered, with only a small depolarization of 2.6 ± 1.5 mV ($n = 7$; $P = 0.3$) when compared to baseline control recordings.

Either during or immediately following the development of the plateau potential, synthetic toxin caused the development of a spontaneous repetitive firing of action potentials with firing frequencies up to 3 Hz (Figure 6B,C). These spontaneous repetitive discharges were not stimulus locked and could not be reversed even by prolonged washing of the preparation with toxin-free solution reflecting the high affinity of the toxin for neurotoxin receptor site-3 (*39*, *40*).

DISCUSSION

The goal of this study was to chemically synthesize the major toxic component, δ-ACTX-Ar1a, of the Sydney funnel-web spider (*A. robustus*) venom and to use this synthetic toxin for further examination of its biological activity. However, a major obstacle in synthesizing pure δ-ACTX-Ar1a was the poor solubility of the reduced peptide in most simple oxidative systems. The addition of 2 M GdnHCL/Tris HCl to the buffer system (containing redox reagents) resulted in some improvement to the solubility, but precipitation was observed over the course of the oxidation. The addition of TFE did not result in any improvement. The addition of 50% 2-propanol did result in a major product, and a substantial increase in the yield of the major product was obtained after predissolving the pure, reduced peptide in a small amount of unbuffered 6 M GdnHCl (apparent pH, 4). The use of silanized glassware and the optimized oxidative conditions resulted in a 10−15% oxidative yield.

Since chemical shift values are dictated by primary sequence and conformation, the essentially identical chemical shifts of naturally occurring and synthetic δ-ACTX-Ar1a confirm that the synthetic δ-ACTX-Ar1a has native sequence, disulfide pairings, and tertiary folding. In particular, the absence of NMR signals for a C-terminal amide group in native δ-ACTX-Ar1a (*27*) and the maintenance of the chemical shifts for the C-terminal Cys^{42} protons between naturally occurring and synthesized δ-ACTX-Ar1a imply that the C-terminus of native δ-ACTX-Ar1a is the same as that of synthetic δ-ACTX-Ar1a, namely, the free acid form.

Under voltage-clamp conditions in DRG neurons, we found that the effects of the synthetic toxin on sodium currents were not significantly different from those previously reported for the native toxin. Neither native nor synthetic δ-ACTX-Ar1a had any effect on TTX-resistant sodium currents, but both exerted a potent selective modulation of TTX-sensitive sodium currents consistent with actions on neurotoxin receptor site-3, including: (a) a slowing of the sodium-channel inactivation; (b) a hyperpolarizing shift in the voltage-dependence of activation; and (c) a hyperpolarizing shift in the steady-state sodium-channel inactivation (h_∞) accompanied by a noninactivating component at prepulse potentials that normally inactivate all TTX-sensitive sodium channels. This indicates that the synthetic toxin shares the complete structural and pharmacological profile of the native toxin.

The successful synthesis and refolding of δ-ACTX-Ar1a provided the opportunity to investigate the effects of

δ-ACTX-Ar1a on resting and action potentials to determine the effects of the toxin on neuronal excitability. Here, we report for the first time that δ-ACTX-Ar1a causes a prolongation of action potential duration, accompanied by spontaneous repetitive firing, but does not depolarize the resting membrane potential. These effects are virtually identical to those reported for δ-ACTX-Hv1a, an ortholog from *H. versuta* venom (*41*), and no doubt underlie the intense muscle fasciculation and autonomic disturbances seen clinically during systemic envenomation. Effects on the autonomic nervous system, including vomiting, profuse sweating, salivation, lachrymation, marked hypertension followed by hypotension, together with effects on the somatic nervous system to cause muscle fasciculation and dyspnoea (*1*), are presumably due to excessive transmitter release. These actions are consistent with the effects of δ-ACTX-Ar1a to cause spontaneous and prolonged prejunctional action potentials in efferent nerve fibers. Moreover, it is these effects that ultimately lead to death from respiratory or circulatory failure (*1*). These alterations in action potential firing and duration are consistent with the modulation of sodium-channel gating and kinetics, to slow inactivation and shift the voltage-dependence of activation, described previously and as previously reported with native toxin (*3*).

The synthetic approach described in this paper provides the means to identify the sodium-channel binding surface (pharmacophore) of δ-ACTX-Ar1a. This can be achieved by synthesizing analogues with selected residue changes, including substitutions with nonnatural amino acids, as has been achieved with other toxins such as ShK, a potassium-channel blocker from the sea anemone *Stichodactyla helianthus* (*42*). Studies with synthetic toxin and analogues will also contribute to a more detailed mapping of site-3, the neurotoxin receptor site on the sodium channel, and provide structure−activity data critical for the determining the phyla-specific actions of this and related atracotoxins.

REFERENCES

1. Sutherland, S. K., and Tibballs, J. (2001) in *Australian Animal Toxins: The Creatures, Their Toxins and Care of the Poisoned Patient*, pp 402−464, Oxford University Press, Melbourne.
2. Nicholson, G. M., and Graudins, A. (2002) *Clin. Exp. Pharmacol. Physiol. 29*, 785−794.
3. Nicholson, G. M., Walsh, R., Little, M. J., and Tyler, M. I. (1998) *Pfluegers Arch. 436*, 117−126.
4. Little, M. J., Zappia, C., Gilles, N., Connor, M., Tyler, M. I., Martin-Eauclaire, M.-F., Gordon, D., and Nicholson, G. M. (1998) *J. Biol. Chem. 273*, 27076−27083.
5. Sutherland, S. K. (1980) *Med. J. Aust. 2*, 437−441.
6. Nicholson, G. M., and Graudins, A. (2003) *J. Toxicol., Toxin Rev. 23*, 81−106.
7. Gregson, R. P., and Spence, I. (1983) *Comp. Biochem. Physiol. C 74*, 125−132.
8. Sheumack, D. D., Baldo, B. A., Carroll, P. R., Hampson, F., Howden, M. E., and Skorulis, A. (1984) *Comp. Biochem. Physiol. C 78*, 55−68.
9. Sheumack, D. D., Claassens, R., Whiteley, N. M., and Howden, M. E. H. (1985) *FEBS Lett. 181*, 154−156.
10. Fletcher, J. I., Chapman, B. E., Mackay, J. P., Howden, M. E. H., and King, G. F. (1997) *Structure 5*, 1525−1535.
11. Brown, M. R., Sheumack, D. D., Tyler, M. I., and Howden, M. E. H. (1988) *Biochem. J. 250*, 401−405.
12. Szeto, T. H., Birinyi-Strachan, L. C., Wang, X.-H., Smith, R., Connor, M., Christie, M. J., King, G. F., and Nicholson, G. M. (2000) *FEBS Lett. 470*, 293−299.
13. Calvete, J. J., Wang, Y., Mann, K., Schafer, W., Niewiarowski, S., and Stewart, G. J. (1992) *FEBS Lett. 309*, 316−320.
14. DeBin, J. A., Maggio, J. E., and Strichartz, G. R. (1993) *Am. J. Physiol. 264*, C361−C369.
15. Pallaghy, P. K., Alewood, D., Alewood, P. F., and Norton, R. S. (1997) *FEBS Lett. 419*, 191−196.
16. Fletcher, J. I., Dingley, A. J., Smith, R., Connor, M., Christie, M. J., and King, G. F. (1999) *Eur. J. Biochem. 264*, 525−533.
17. Pallaghy, P. K., Neilsen, K. J., Craik, D. J., and Norton, R. S. (1994) *Protein Sci. 3*, 1833−1839.
18. Maggio, F., and King, G. F. (2002) *J .Biol. Chem. 277*, 22806−22813.
19. Nishio, H., Kumagaye, K. Y., Kubo, S., Chen, Y. N., Momiyama, A., Takahashi, T., Kimura, T., and Sakakibara, S. (1993) *Biochem. Biophys. Res. Commun. 196*, 1447−1453.
20. Bodi, J., Nishio, H., Zhou, Y., Branton, W. D., Kimura, T., and Sakakibara, S. (1995) *Pept. Res. 8*, 228−235.
21. Kuroda, H., Chen, Y. N., Watanabe, T. X., Kimura, T., and Sakakibara, S. (1992) *Pept. Res. 5*, 265−268.
22. Kharrat, R., Mabrouk, K., Crest, M., Darbon, H., Oughideni, R., Martin-Eauclaire, M. F., Jacquet, G., el Ayeb, M., Van Rietschoten, J., Rochat, H., and Sabatier, J. M. (1996) *Eur. J. Biochem. 242*, 491−498.
23. Sabatier, J. M., Darbon, H., Fourquet, P., Rochat, H., and Van Rietschoten, J. (1987) *Int. J. Pept. Protein Res. 30*, 125−134.
24. Schneider, J., and Kent, S. B. (1988) *Cell 54*, 363−368.
25. Torres, A., Bansal, P., Alewood, P. F., Kuchel, P., and Vandenberg, J. (2003) *FEBS Lett., 539*, 138−142.
26. Nielsen, K. J., Alewood, D., Andrews, J., Kent, S. B., and Craik, D. J. (1994) *Protein Sci. 3*, 291−302.
27. Temple, M. D., Hinds, M. G., Sheumack, D. D., Howden, M. E., and Norton, R. S. (1999) *Toxicon 37*, 485−506.
28. Sawyer, T. K., Pals, D. T., Mao, B., Staples, D. J., de Vaux, A. E., Maggiora, L. L., Affholter, J. A., Kati, W., Duchamp, D., Hester, J. B. et al. (1988) *J. Med. Chem. 31*, 18−30.
29. Sarin, V. K., Kent, S. B., Tam, J. P., and Merrifield, R. B. (1981) *Anal. Biochem. 117*, 147−157.
30. Russell, J., McKeown, J. A., Hensman, C., Smith, W. E., and Reglinski, J. (1997) *J. Pharm. Biomed. Anal. 15*, 1757−1763.
31. Sklenar, V., Peterson, R. D., Rejante, M. R., and Feigon, J. (1993) *J. Biomol. NMR 3*, 721−727.
32. Nicholson, G. M., Willow, M., Howden, M. E. H., and Narahashi, T. (1994) *Pfluegers Arch. 428*, 400−409.
33. Hamill, O. P., Marty, A., Neher, E., Sakmann, B., and Sigworth, F. J. (1981) *Pfluegers Arch. 391*, 85−100.
34. Ogata, N., Nishimura, M., and Narahashi, T. (1989) *J. Pharmacol. Exp. Ther. 248*, 605−613.
35. Roy, M. L., and Narahashi, T. (1992) *J. Neurosci. 12*, 2104−2111.
36. Bezanilla, F., and Armstrong, C. M. (1977) *J. Gen. Physiol. 70*, 594−566.
37. Strichartz, G. R., and Wang, G. K. (1986) *J. Gen. Physiol. 88*, 413−435.
38. Wasserstrom, J. A., Kelly, J. E., and Liberty, K. N. (1993) *Pfluegers Arch. 424*, 15−24.
39. Little, M. J., Wilson, H., Zappia, C., Cestèle, S., Tyler, M. I., Martin-Eauclaire, M.-F., Gordon, D., and Nicholson, G. M. (1998) *FEBS Lett. 439*, 246−252.
40. Gilles, N., Harrison, G., Karbat, I., Gurevitz, M., Nicholson, G. M., and Gordon, D. (2001) *Eur. J. Biochem. 269*, 1500−1510.
41. Grolleau, F., and Lapied, B. (2000) *J. Exp. Biol. 203*, 1633−1648.
42. Kalman, K., Pennington, M. W., Lanigan, M. D., Nguyen, A., Rauer, H., Mahnir, V., Paschetto, K., Kem, W. R., Grissmer, S., Gutman, G. A., Christian, E. P., Cahalan, M. D., Norton, R. S., and Chandy, K. G. (1998) *J. Biol. Chem. 273*, 32697−32707.

BI030091N